AGU PUBLICATIONS

Geophysical Research Letters

RESEARCH LETTER
10.1002/2016GL070088

Key Points:
- We identify and describe eight resonant modes of Rainbow Bridge, Utah, between 1 and 6 Hz
- Lake Powell, like other lakes in Utah, generates seismic energy around 1 Hz from wave action
- The lake microseism and a distant induced earthquake stimulated low-level resonance of the bridge

Supporting Information:
- Supporting Information S1
- Movie S1
- Movie S2
- Movie S3
- Movie S4

Correspondence to:
J. R. Moore,
jeff.moore@utah.edu

Citation:
Moore, J. R., M. S. Thorne, K. D. Koper, J. R. Wood, K. Goddard, R. Burlacu, S. Doyle, E. Stanfield, and B. White (2016), Anthropogenic sources stimulate resonance of a natural rock bridge, *Geophys. Res. Lett.*, *43*, 9669–9676, doi:10.1002/2016GL070088.

Received 17 JUN 2016
Accepted 6 SEP 2016
Accepted article online 21 SEP 2016
Published online 24 SEP 2016

Anthropogenic sources stimulate resonance of a natural rock bridge

Jeffrey R. Moore[1], Michael S. Thorne[1], Keith D. Koper[1], John R. Wood[2], Kyler Goddard[1], Relu Burlacu[1], Sarah Doyle[3], Erik Stanfield[3], and Benjamin White[1]

[1]Department of Geology and Geophysics, University of Utah, Salt Lake City, Utah, USA, [2]Geologic Resources Division, National Park Service, Lakewood, Colorado, USA, [3]Glen Canyon National Recreation Area, National Park Service, Page, Arizona, USA

Abstract The natural modes of vibration of bedrock landforms, as well as the sources and effects of stimulated resonance remain poorly understood. Here we show that seismic energy created by an induced earthquake and an artificial reservoir has spectral content coincident with the natural modes of vibration of a prominent rock bridge. We measured the resonant frequencies of Rainbow Bridge, Utah using data from two broadband seismometers placed on the span, and identified eight distinct vibrational modes between 1 and 6 Hz. A distant, induced earthquake produced local ground motion rich in 1 Hz energy, stimulating a 20 dB increase in measured power at the bridge's fundamental mode. Moreover, we establish that wave action on Lake Powell, an artificial reservoir, generates microseismic energy with peak power ~1 Hz, also exciting resonance of Rainbow Bridge. These anthropogenic sources represent relatively new energy input for the bridge with unknown consequences for structural fatigue.

1. Introduction

Vibration sources rich in energy at a structure's natural frequencies can excite resonance, resulting in increased amplitude oscillations and potential internal damage [*Carder*, 1936; *Hall et al*., 1995]. While analysis of structural dynamics is well developed in civil engineering [*Chopra*, 2011], until recently the same methodology has not been applied to naturally occurring geological features such as rock arches, which may exhibit similar natural modes [*Lévy et al*., 2010; *Burjánek et al*., 2012; *Bottelin et al*., 2013; *Starr et al*., 2015]. Like civil structures, resonance of rock features may be stimulated by a variety of sources; however, in contrast, natural structures are not specifically designed to accommodate the variety or periodicity of human-induced loads. Here we evaluate the dynamics of one of the world's longest rock spans, Rainbow Bridge, Utah [*Chidsey et al*., 2000], identifying key natural frequencies as well as anthropogenic sources that stimulate resonance.

Situated aside Lake Powell near the Arizona-Utah border (Figure 1), Rainbow Bridge is a sacred site for neighboring Native American tribes and is an internationally recognized visitor attraction managed as a National Monument by the U.S. National Park Service [*Sproul*, 2001]. The natural bridge has an opening breadth of 83 m and vertical height of 75 m as it crosses Bridge Creek [*Skipper*, 1985]. At full pool, water from Lake Powell extends underneath the bridge; however as lake levels vary the shoreline can be up to 1 km away. Concerns regarding adverse anthropogenic effects (e.g., rising waters of Lake Powell) have prompted several past studies [*Halliday and Woodbury*, 1961; *Dames and Moore Group*, 1972; *Skipper*, 1985]. However, previous investigations have not probed the structural dynamics of Rainbow Bridge, including analysis of anthropogenic energy sources, which was the focus of our work.

Structures at the Earth's surface vibrate in response to the ambient wavefield and boundary layer effects. Energy sources may be natural, such as wind and earthquakes, or anthropogenic, such as traffic or machinery [*Nakamura*, 1989; *Clinton et al*., 2006; *Bonnefoy-Claudet et al*., 2006]. Human activity has altered the Earth's vibration wavefield, for example, by generating moderate-magnitude-induced earthquakes at frequent intervals [*Keranen et al*., 2014], air and ground pressure waves from blasting or aircraft overflights [*Hanson et al*., 1991], or persistent background vibration from transit sources [*Hanson et al*., 2006]. However, the dynamic response of geological features (e.g., rock arches) to the variety of anthropogenic energy sources is largely unknown. Moreover, potential impacts of this vibrational energy are rarely considered in stability analysis of natural landforms [cf. *King*, 2001; *King and DeMarco*, 2003].

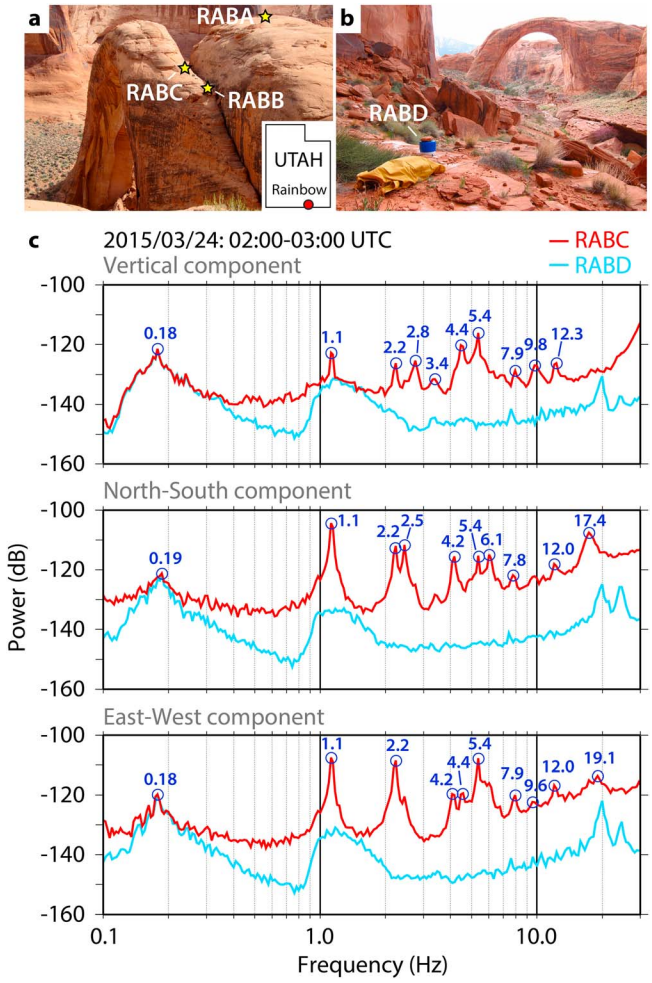

Figure 1. Ambient vibration field study and results. (a) Rainbow Bridge viewed from the west (inset location) showing seismometer positions RABA, RABB, and RABC. (b) View from the north showing reference seismometer RABD. (c) Power spectral density plots for sensors RABC (red) on the bridge and reference RABD (blue) for a selected 1 h time period exhibiting typical results; peak frequencies labeled. Power is reported in decibel (dB) units of spectral ground acceleration, $10\log_{10}$ ($m^2/s^4/Hz$).

2. Experimental Data and Results

We conducted a field test on 23–24 March 2015 to measure the resonant frequencies of Rainbow Bridge from ambient seismic data. We deployed four Nanometrics Trillium Compact three-component broadband seismometers with 24 bit Centaur digitizers recording continuous data at 100 Hz (Figure 1): (1) station RABA was located 25 m from Rainbow Bridge on an adjoining rock knoll, (2) RABB was located on the bridge at the western abutment, (3) RABC was placed on the lintel at our farthest accessible position, and (4) RABD was located in the canyon bottom 220 m to the northwest. Due to safety concerns, we could not access additional sensor positions on the bridge. All seismometers were placed on solid, bare rock surfaces, aligned to magnetic north, and leveled. The maximum duration of recording was 22 h, limited by access constraints on this highly visited and revered natural bridge.

Ambient seismic data were processed for spectral content, degree of polarization, and orientation. We (1) removed the mean and trend from each trace, (2) removed the instrument response by spectral division, and (3) bandpass filtered these data between 0.002 and 50 Hz. We then computed the power spectral density (PSD) by fast Fourier transform over hour-long data blocks subdivided into sixteen 409.6 s windows with 50% overlap and averaged the PSD [*Koper and Burlacu*, 2015] to reduce the variance in the spectrum. For polarization analysis we measured polarization attributes at distinct resonant frequencies [*Koper and Hawley*, 2010]. We calculated the degree of polarization (dimensionless ranging from 0 to 1), the orientation of motion in the horizontal plane (azimuth clockwise from magnetic north), and the dip of particle motion (degrees from horizontal). The duration of data analyzed at each sensor was (UTC): RABA: 23 March 21:00 to 24 March 19:00, RABB: 23 March 23:00 to 24 March 19:00; RABC: 23 March 23:00 to 24 March 19:00; RABD: 24 March 01:00 to 24 March 17:00.

Figure 1 compares spectra from station RABC on the bridge with those from reference station RABD on the canyon floor. We observed several consistent spectral peaks between 1 and 10 Hz at RABC that were not present on the reference sensor, notably at 1.1, 2.2, 2.5, 4.2, 4.4, 5.4, 6.1, 7.9, and 9.8 Hz, which we interpret as resonant frequencies of Rainbow Bridge. Energy at frequencies greater than 10 Hz was less consistent over the period of our test and challenging to interpret. Spectra from station RABA revealed strong peaks at 2.7 and 3.4 Hz, which likely represent natural modes of the adjoining knoll, while spectra from station RABB reflected combined vibration of the bridge and knoll. An additional spectral peak observed in all data

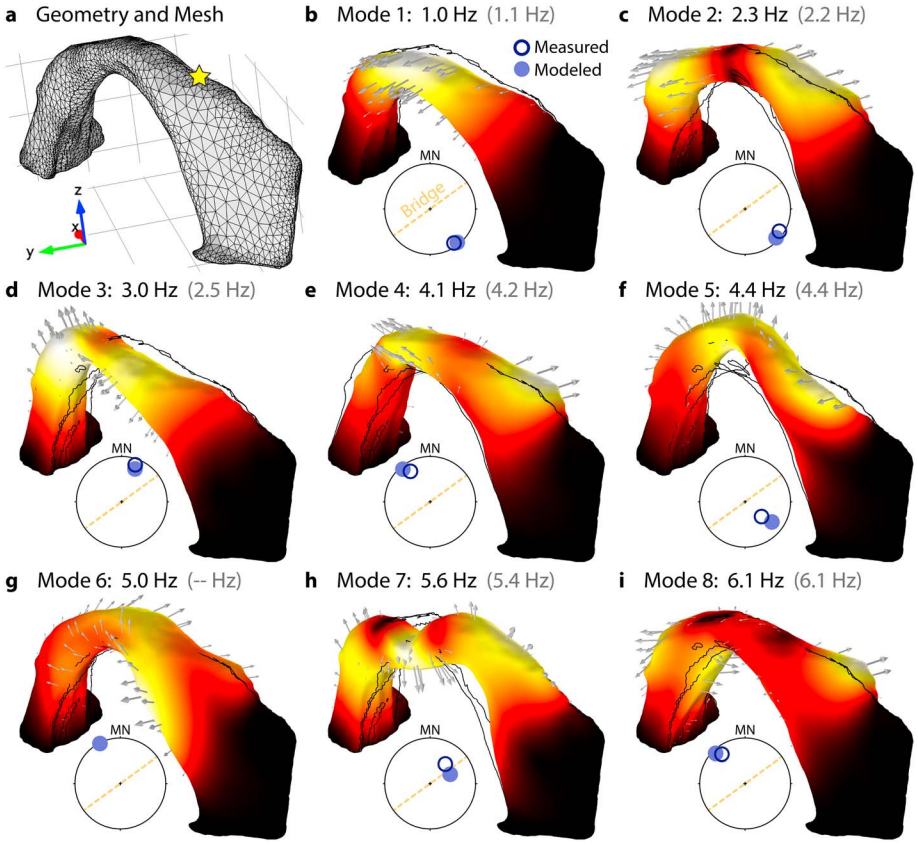

Figure 2. Numerical modal analysis of Rainbow Bridge. (a) Geometry and finite element mesh; *y* (magnetic north) and *z* (vertical) grid spacing = 20 m, *x* (east) grid spacing = 50 m. (b)–(i) First eight modes of vibration with accompanying eigenfrequency; measured values shown in parentheses. Color map, deformed body, and arrows illustrate deformation at zero phase (normalized relative scale for each mode), wireframe shows static form. Stereo plots compare measured (open circles) and modeled (filled) polarization vectors (see also Table 1); trend of Rainbow Bridge indicated by dashed line. MN = magnetic north.

occurred at ~0.18 Hz, which is the microseism related to ocean-generated seismic waves [*Longuet-Higgins*, 1950]. The peak near 1 Hz evident at RABD is discussed later in section 4.

At the fundamental frequency of 1.1 Hz, vibration is strongly polarized and oriented perpendicular to the trend of the bridge (Figure 2 and Table 1). Particle motion at several higher resonant frequencies (2.2, 4.2, 4.4, and 6.1 Hz) shares similar attributes, with strongly polarized, predominantly horizontal ground motion

Table 1. Comparison of Measured and Modeled Eigenmodes at Sensor Position RABC[a]

Mode	Measured Frequency (Hz)	Degree of Polarization [0–1]	Measured Azimuth (deg)	Measured Incidence (deg)	Modeled Frequency (Hz)	Modeled Azimuth (deg)	Modeled Incidence (deg)	Maximum Mass Participation (%)
1	1.1	1.0	145	85	1.0	141	87	29.3 (N)
2	2.2	0.9	123	84	2.3	133	86	2.0 (N)
3	2.5	0.8	20	82	3.0	22	76	28.8 (E)
4	4.2	0.8	147	78	4.1	140	87	9.1 (Z)
5	4.4	0.6	132	52	4.4	127	73	26.5 (Z)
6	-	-	-	-	5.0	153	89	3.9 (Z)
7	5.4	0.5	38	57	5.6	65	52	5.2 (Z)
8	6.1	0.9	141	79	6.1	135	86	0.2 (E)

[a]Azimuth: degrees from magnetic north. Incidence: degrees from vertical. Direction of maximum mass participation indicated in parentheses.

oriented subperpendicular to the bridge. Meanwhile, vibration at 2.5 and 5.0 Hz is aligned subparallel to the bridge. Frequency wander over the 20 h period of data collection at RABC was generally not observed; only the 2.5 and 5.0 Hz peaks drifted slowly (by a few percent) but without clear relation to environmental changes [cf. *Bottelin et al*., 2013]. Strong winds in the beginning of our test (strong enough to blow over our portable wind sensor) generated the highest spectral amplitudes on the bridge, but did not change the resonant frequencies.

3. Numerical Modal Analysis

To better understand the resonant modes of Rainbow Bridge, we performed three-dimensional numerical modal analysis. Input parameters for the model included the geometry of the bridge, mechanical boundary conditions, and material properties. In total, 100 modes were analyzed in order to reach 90% total mass participation in each orthogonal direction [*American Society of Civil Engineers*, 2003]; however, in practice, only a few of these modes are significant (here defined as including $>2\%$ of the total bridge mass, 1.0×10^8 kg, in any cardinal direction).

We rendered a photogrammetric model of Rainbow Bridge as input for modal analysis. Data were obtained using a Nikon D800 DSLR camera and a differential Global Navigation Satellite Systems (GNSS) receiver. Camera placement followed a path that roughly encircled the span, and photographs acquired images with minimally one-third overlap [*Matthews*, 2008]. Spatial data for each camera placement were recorded by the GNSS receiver. We used AGISoft PhotoScan Professional (www.agisoft.com) for photograph alignment, point cloud refinement, and creation of the georeferenced 3-D surface model (Figure S1 in the supporting information). Photographic coverage of the bridge was not complete, which resulted in holes on the upper surface of the model. We used MeshMixer (www.meshmixer.com) to close these holes and render a realistic and uniform surface model (Figure S2). Cumulative georeferencing error of our final model was ±8.2 cm. Confidence in model scaling is highlighted by our opening-breadth measurement of 83.4 m, which is close to the value of 83.8 m obtained by a previous Bureau of Reclamation survey [*Sproul*, 2001].

Numerical modal analysis was performed using the finite element software COMSOL Multiphysics (www.comsol.com). Mechanical boundary conditions were determined from field assessment; most model boundaries were free to move while the bases of the bridge abutments were fixed. The crack separating the bridge from the adjacent knoll (see Figure 1) presented the largest unknown boundary condition, which we characterized through visual field inspection and fixed select faces of the interior crack walls accordingly (see Figure S2). For material properties, we assumed a uniform density for Navajo sandstone of 2000 kg/m^3 based on past reported values from Rainbow Bridge test specimens [*Dames and Moore Group*, 1972] and then varied Young's modulus (E) to achieve the best fit with measured resonant frequencies. $E = 4.7$ GPa provided optimum match to measured frequencies, which is within the range of nominal values for a weathered sandstone rock mass [*Hoek and Diederichs*, 2006] and similar to the value used for another natural arch in Navajo sandstone (5.5 GPa) [*Starr et al*., 2015].

We show the first eight eigenmodes of Rainbow Bridge in Figure 2 (see also Movie S1). Mode 1, the fundamental mode of vibration, is modeled at 1.0 Hz and represents the first out-of-plane bending mode (i.e., perpendicular flexure), while mode 2, modeled at 2.3 Hz, represents the second out-of-plane bending mode, consistent with measured polarization orientations (Figure 2 and Table 1). Mode 3 represents in-plane bending, as also evidenced by experimental polarization results. Several additional in- and out-of-plane bending modes are present, as well as a torsional mode (mode 6) at 5.0 Hz that does not explicitly appear in our field data but occurs at a similar frequency as mode 7 and thus may be masked. This mode may be detected in field data with additional available sensor positions [e.g., *Michel et al*., 2008; *Poggi et al*., 2015].

The overall agreement between measured and modeled eigenfrequencies and polarization vectors is excellent, confirming that peak frequencies identified in our experimental data (Figure 1) are resonant frequencies of Rainbow Bridge. We consider values within ±10% of measurements to be a good match; however, our results rely on underlying assumptions of uniform material properties and a lack of discontinuities within the bridge. Our analysis also assumes that Rainbow Bridge is a singular solid feature, and thus does not model superposed vibration from near-surface slabs or other partly detached portions. Despite these strong simplifications, numerical modal analysis reproduced experimental data well and added valuable detail to our understanding of key resonant modes.

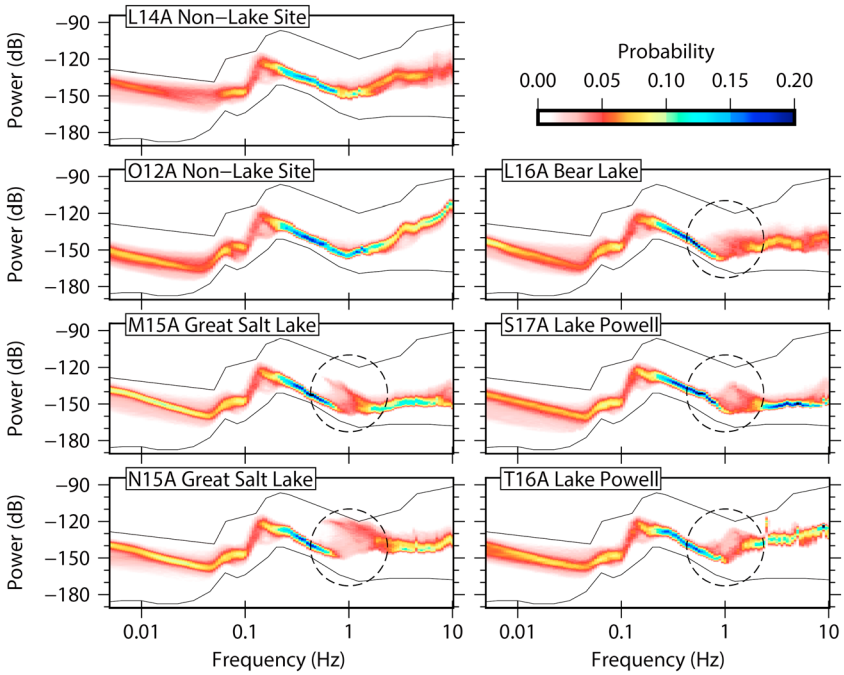

Figure 3. Probability density functions for seven seismic stations in Utah. Stations L14A and O12A are not located near lakes and lack anomalous energy around 1 Hz. Stations M15A and N15A are located next to the Great Salt Lake, L16A is next to Bear Lake, while stations S17A and T16A are located next to Lake Powell. All lake-proximal stations show anomalous energy in the 0.9–1.8 Hz band (dashed circles). Power is reported in decibel (dB) units of spectral ground acceleration, $10\log_{10}$ (m^2/s^4/Hz). High- and low-noise models from *Peterson* [1993] are shown in each panel.

4. Sources Stimulating Resonance

The persistent spectral peak observed between 0.9 and 1.8 Hz on all sensors, including the reference sensor (Figure 1), is unexpected because global models of Earth's ambient noise field show a local minimum in spectral power at these frequencies [*Peterson*, 1993; *Berger et al*., 2004]. To determine if this peak is a persistent feature of the regional ambient wavefield, we examined seismic noise at 112 three-component broadband stations in the Utah region using frequency-dependent polarization analysis (Figure S3). Of the 112 stations, 85 were deployed for 18–24 months during 2006–2010 as part of the Transportable Array (TA) experiment of USArray, and 27 are permanent stations in the University of Utah Regional Seismic Network.

Frequency-dependent polarization analysis [*Koper and Hawley*, 2010] was applied to continuous data recorded at TA stations [*Koper and Burlacu*, 2015] and UU stations [*Goddard et al*., 2014]. Station locations and operating epochs for all of the instruments are available from IRIS (www.iris.edu/mda). For each hour of data at each station, the frequency-dependent 3×3 spectral matrix was computed and decomposed into eigenvalues and eigenvectors. Polarization information was obtained from the dominant eigenvector [*Park et al*., 1987], and the dominant eigenvalue [*Wagner and Owens*, 1996] was used to estimate the power spectral density (PSD). Time averaging was achieved with 10 tapered, overlapping subwindows within each hour, and frequency averaging was achieved within bins equally spaced in $\log_{10}$ space [*Koper and Burlacu*, 2015].

For each station, we combined thousands of individual PSD estimates into a 2-D probability density function (PDF), using every viable hour of available data [*McNamara and Buland*, 2004]. Fourteen of the PDFs show anomalous energy in the 0.9–1.8 Hz band (Figures 3 and S4). All stations demonstrating this anomalous feature are near large lakes in Utah (most within 10 km), including three TA stations located near Lake Powell. We infer that this energy is created by lake-induced microseisms and that its shorter period relative to ocean-generated microseisms is caused by the smaller surface area of the lakes, which limits the fetch available for wind-driven wave action [*Webb*, 1998]. As the band of this anomalous energy coincides with the anomalous energy observed on all our sensors, we further infer that this lake microseism is recorded at Rainbow Bridge. Although less common than ocean-generated microseisms, lake-generated microseisms have

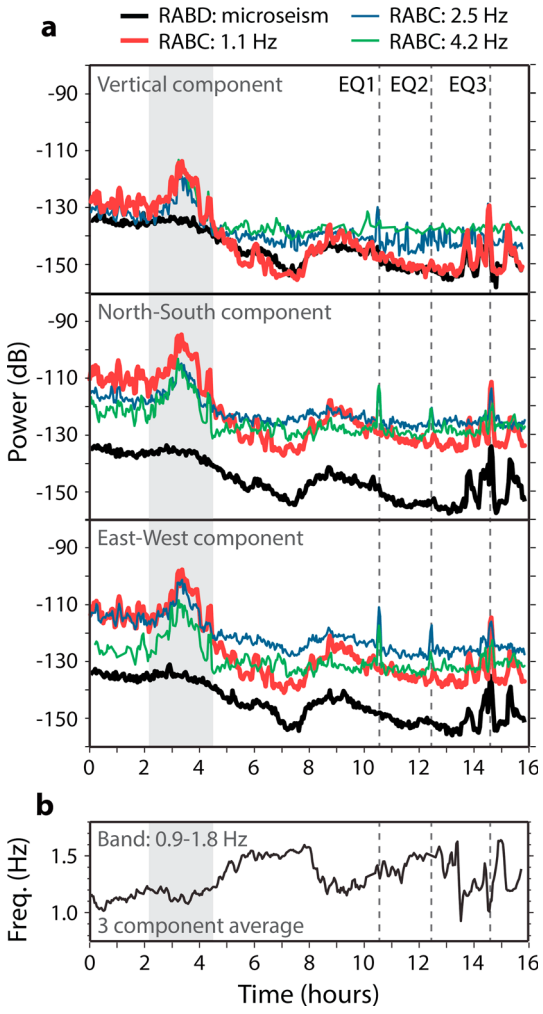

Figure 4. Time evolution of Rainbow Bridge spectra. (a) Peak Power Spectral Density (PSD) over time for mode 1 (red), mode 3 (blue), and mode 4 (green) measured at RABC. Peak PSD for the lake microseism (0.9–1.8 Hz) measured at RABD is shown in black. Power is reported in decibel (dB) units of spectral ground acceleration, $10\log_{10}$ (m^2/s^4/Hz). (b) Peak frequency of the lake microseism over time measured at RABD, averaged over the three components of motion. Gray-shaded area corresponds to a period of strong winds, while the dashed lines indicate the times of three regional earthquakes. Start of the record is 24 March 2015 0:100 UTC.

previously been observed from the Great Lakes [*Lynch*, 1952; *Kerman and Mereu*, 1993] and the Great Slave Lake [*Weichert and Henger*, 1976; *Koper et al.*, 2009].

The interplay between natural and anthropogenic vibration sources is demonstrated in Figure 4a (see also Movies S2–S4), which shows the time evolution of peak power for select eigenmodes at RABC compared to the peak power of the lake microseism at RABD (hereafter the lake microseism). At the beginning of our test, power of mode 1 on the vertical component is slightly elevated above the lake microseism, whereas the horizontal components are 18–28 dB greater. Modes 3 and 4 are similar. Strong canyon winds were present between ~2 and 4 h (shaded region in Figure 4a, evidenced from limited on-site wind data and personal observation at a nearby location), and the power of all modes rises by ~16 dB. However, the power of the lake microseism remains relatively unchanged, indicating that canyon winds predominantly excite resonance of the bridge.

At ~5 h into our test, canyon winds die down and power on all modes, as well as the lake microseism, decreases. However, while the power of mode 1 closely tracks the lake microseism, the power of higher modes does not decrease accordingly. In addition, the broad spectral peak of the lake microseism narrows and migrates to higher frequencies (Figure 4b). As this value increases, the power of the vertical component of mode 1 decreases below the peak power of the lake microseism, ostensibly because mode 1 is no longer being forced by the lake. Between 8 and 10 h, the power of the lake microseism increases and its dominant frequency migrates back to near 1.1 Hz. This increase is mimicked by mode 1 resonance of Rainbow Bridge, whereas power at higher modes remains relatively constant. The last several hours of our test were calm, and the power of mode 1 and the lake microseism decrease, while power at higher modes remains steady.

During the final hours of our experiment, we recorded three regional earthquakes (Table S1 and Figures S5–S7); the first two (*M*1.5 and *M*1.7) were located in south-central Utah, while the third (*M*3.7) was likely an induced earthquake located near the Oklahoma-Kansas border [*Rubinstein and Mahani*, 2015]. Each earthquake generated a transient increase in power at the resonant frequencies of Rainbow Bridge of up to 20 dB (factor of 10 increase in amplitude) (Figure 4). The two closer earthquakes were enriched in high-frequency energy, exciting resonance of the bridge primarily at higher modes, while the

third earthquake, being farther away (~1000 km) and of larger magnitude, was relatively rich in ~1 Hz energy and stimulated an increase in power at the bridge's fundamental mode. No change in resonant frequencies was observed during or after these earthquakes.

5. Conclusions

We measured the resonant frequencies of Rainbow Bridge, Utah, one of the world's longest rock spans, in a field experiment recording ambient vibration data. Measurements were generated over ~20 h using two broadband three-component seismometers placed on the bridge and compared to concurrent data from nearby reference stations 20 and 220 m distant. We identified seven distinct modes of vibration for Rainbow Bridge between 1 and 6 Hz, with the fundamental frequency at 1.1 Hz. Data for each resonant frequency were analyzed to determine the frequency-dependent polarization vector in order to clarify mode shapes; e.g., the fundamental mode represents out-of-plane flexure. We then compared experimental data to results of 3-D numerical modal analysis, using a new photogrammetric model of Rainbow Bridge generated in this study. Results compare well with measured data for seven of the first eight modeled modes, matching eigenfrequencies and eigenvectors generally within 10% and providing valuable detail on the complete displacement field for each mode.

We show that seismic energy created by waves in an artificial reservoir, as well as an induced earthquake, has spectral content coincident with the natural modes of Rainbow Bridge and can excite resonance. Resulting vibrations, while small, contribute to increased rates of microseismic energy uptake, which is a new condition in the life cycle of a natural structure. The presence of Lake Powell, for example, maintains fundamental mode vibration of Rainbow Bridge at higher levels than in its absence. The long-term impact of this added energy on the structural health of any geological feature is ultimately unknown; however, we hypothesize that sustained microseismic vibrations may in some cases contribute to fatigue of critically stressed crack tips, in combination with damage from infrequent high-magnitude vibration events [*Brain et al.*, 2014; *Gischig et al.*, 2015]. Further study of the structural effects of microseismic vibrations may be warranted.

Acknowledgments

We thank the following tribal organizations for motivating this study and allowing access to Rainbow Bridge: Navajo Nation, Hopi Tribe, Kiabab Paiute Tribe, San Juan Southern Paiute Tribe, White Mesa Ute, and the Pueblo of Zuni. We gratefully acknowledge the University of Utah Center for High Performance Computing for providing computational resources. Data generated and analyzed are available from http://geohazards.earth.utah.edu/data.html and http://ds.iris.edu/mda. This study was funded by the National Park Service. J.R.M and M.S.T are additionally supported by the National Science Foundation grant EAR-1424896. Clotaire Michel and an anonymous reviewer provided helpful comments that improved this manuscript.

References

American Society of Civil Engineers (2003), Minimum design loads for buildings and other structures (SEI/ASCE 7-02), *Am. Soc. Civ. Eng.*, doi:10.1061/9780784406243.

Berger, J., P. Davis, and G. Ekström (2004), Ambient Earth noise: A survey of the Global Seismographic Network, *J. Geophys. Res.*, *109*, B11307, doi:10.1029/2004JB003408.

Bonnefoy-Claudet, S., F. Cotton, and P. Y. Bard (2006), The nature of noise wavefield and its applications for site effects studies: A literature review, *Earth Sci. Rev.*, *79*(3–4), 205–227.

Bottelin, P., C. Lévy, L. Baillet, D. Jongmans, and P. Guéguen (2013), Modal and thermal analysis of Les Arches unstable rock column (Vercors massif, French Alps), *Geophys. J. Int.*, *194*, 849–858, doi:10.1093/gji/ggt046.

Brain, M. J., N. J. Rosser, E. C. Norman, and D. N. Petley (2014), Are microseismic ground displacements a significant geomorphic agent?, *Geomorphology*, *207*, 161–173, doi:10.1016/j.geomorph.2013.11.002.

Burjánek, J., J. R. Moore, F. X. Yugsi-Molina, and D. Fäh (2012), Instrumental evidence of normal mode rock slope vibration, *Geophys. J. Int.*, *188*, 559–569, doi:10.1111/j.1365-246X.2011.05272.x.

Carder, D. S. (1936), Observed vibrations of buildings, *Bull. Seismol. Soc. Am.*, *26*(3), 245–277.

Chidsey, T. C., Jr., G. C. Willis, D. A. Sprinkel, and P. B. Anderson (2000), Geology of Rainbow Bridge National Monument, Utah, in *Geology of Utah's Parks and Monuments*, vol. 28, edited by D. A. Sprinkel, T. C. Chidsey Jr., and P. B. Anderson, pp. 251–262, Utah Geological Association, Salt Lake.

Chopra, A. K. (2011), *Dynamics of Structures*, 4th ed., 992 pp., Prentice Hall, Upper Saddle River, N J.

Clinton, J. F., S. C. Bradford, T. H. Heaton, and J. Favela (2006), The observed wander of the natural frequencies in a structure, *Bull. Seismol. Soc. Am.*, *96*, 237–257, doi:10.1785/0120050052.

Dames & Moore Group (1972), Geological and structural evaluation of Rainbow Bridge, Rainbow Bridge National Monument, Unpublished consultant's report to the Upper Colorado River Commission, Salt Lake.

Gischig, V., G. Preisig, and E. Eberhardt (2015), Numerical investigation of seismically induced rock mass fatigue as a mechanism contributing to the progressive failure of deep-seated landslides, *Rock Mech. Rock Eng.*, *49*(6), 2457–2478.

Goddard, K., K. D. Koper, and R. Burlacu (2014), Microseisms from the Great Salt Lake, Abstract S41A-4444 presented at 2014 Fall Meeting, AGU, San Francisco, Calif., 15-19 Dec.

Hall, J. F., T. H. Heaton, M. W. Halling, and D. J. Wald (1995), Near-source ground motion and its effects on flexible buildings, *Earthquake Spectra*, *11*, 569–605.

Halliday, W. R., and A. M. Woodbury (1961), Protection of Rainbow Bridge National Monument, *Science*, *133*, 1572–1583.

Hanson, C. E., K. W. King, M. E. Eagan, and R. D. Horonjeff (1991), Aircraft noise effects on cultural resources: Review of technical literature, NPOA Report 91–3, National Park Service contract report.

Hanson, C. E., D. A. Towers, and L. D. Meister (2006), Transit noise and vibration impact assessment, U.S. Department of Transportation Federal Transit Administration report FTA-VA-90-1003-06.

Hoek, E., and M. S. Diederichs (2006), Empirical estimation of rock mass modulus, *Int. J. Rock Mech. Min. Sci.*, *43*, 203–215, doi:10.1016/j.ijrmms.2005.06.005.

Keranen, K. M., M. Weingarten, G. A. Abers, B. A. Bekins, and S. Ge (2014), Sharp increase in central Oklahoma seismicity since 2008 induced by massive wastewater injection, *Science*, *345*, 448–451, doi:10.1126/science.1255802.
Kerman, B. R., and R. F. Mereu (1993), Wind-induced microseisms from Lake Ontario, *Atmos. Ocean*, *31*, 501–516.
King, K. W. (2001), Chiricahua pinnacle vibration investigation, National Park Service contract report.
King, K. W., and M. J. DeMarco (2003), Impacts of construction vibrations on rock pinnacles and natural bridges, General Hitchcock Highway, Tucson, AZ, Proceedings Third International Conference on Applied Geophysics, Orlando, FL.
Koper, K. D., and R. Burlacu (2015), The fine structure of double-frequency microseisms recorded by seismometers in North America, *J. Geophys. Res. Solid Earth*, *120*, 1677–1691, doi:10.1002/2014JB011820.
Koper, K. D., and V. L. Hawley (2010), Frequency dependent polarization analysis of ambient seismic noise recorded at a broadband seismometer in the central United States, *Earthquake Sci.*, *23*, 439–447, doi:10.1007/s11589-010-0743-5.
Koper, K. D., B. de Foy, and H. Benz (2009), Composition and variation of noise recorded at the Yellowknife Seismic Array, 1991–2007, *J. Geophys. Res.*, *114*, B10310, doi:10.1029/2009JB006307.
Lévy, C., L. Baillet, D. Jongmans, P. Mourot, and D. Hantz (2010), Dynamic response of the Chamousset rock column (Western Alps, France), *J. Geophys. Res.*, *115*, F04043, doi:10.1029/2009JF001606.
Longuet-Higgins, M. S. (1950), A theory of the origin of microseisms, *Philos. Trans. R. Soc. London Ser. A Math. Phys. Sci.*, *243*, 1–35.
Lynch, J. (1952), The Great Lakes, a source of two-second frontal microseisms, *Eos Trans. AGU*, *33*, 432–434.
Matthews, N. A. (2008), Aerial and close-range photogrammetric technology: Providing resource documentation, interpretation and preservation, Technical Note 428, U.S. Department of the Interior, Bureau of Land Management, Denver, Colo.
McNamara, D. E., and R. P. Buland (2004), Ambient noise levels in the continental United States, *Bull. Seismol. Soc. Am.*, *94*, 1517–1527.
Michel, C., P. Guéguen, and P. Y. Bard (2008), Dynamic parameters of structures extracted from ambient vibration measurements: An aid for the seismic vulnerability assessment of existing buildings in moderate seismic hazard regions, *Soil Dynam. Earthquake Eng.*, *28*(8), 593–604.
Nakamura, Y. (1989), *A Method for Dynamic Characteristics Estimation of Subsurface Using Microtremor on the Ground Surface*, vol. 30, pp. 25–33, Quarterly Report of Railway Technical Research Institute (RTRI), Tokyo.
Park, J., F. L. Vernon, and C. R. Lindberg (1987), Frequency dependent polarization analysis of high-frequency seismograms, *J. Geophys. Res.*, *92*, 12,664–12,674, doi:10.1029/JB092iB12p12664.
Peterson, J. (1993), Observations and modeling of seismic background noise, Open-File Report 93-322, U.S. Department of Interior, Geological Survey, Albuquerque, New Mexico.
Poggi, V., L. Ermert, J. Burjanek, C. Michel, and D. Fäh (2015), Modal analysis of 2-D sedimentary basin from frequency domain decomposition of ambient vibration array recordings, *Geophys. J. Int.*, *200*(1), 615–626.
Rubinstein, J. L., and A. B. Mahani (2015), Myths and facts on wastewater injection, hydraulic fracturing, enhanced oil recovery, and induced seismicity, *Seismol. Res. Lett.*, *86*, 1060–1067, doi:10.1785/0220150067.
Skipper, K. J. (1985), Rainbow Bridge National Monument monitoring program: Final status report, U.S. Dept. of Interior, Bureau of Reclamation, Salt Lake.
Sproul, D. K. (2001), *A Bridge Between Cultures: An Administrative History of Rainbow Bridge National Monument*, U.S. Dept. of the Interior, National Park Service, Denver, Colo.
Starr, A. M., J. R. Moore, and M. S. Thorne (2015), Ambient resonance of Mesa Arch, Canyonlands National Park, Utah, *Geophys. Res. Lett.*, *42*, 6696–6702, doi:10.1002/2015GL064917.
Wagner, G. S., and T. J. Owens (1996), Signal detection using multi-channel seismic data, *Bull. Seismol. Soc. Am.*, *86*, 221–231.
Webb, S. (1998), Broadband seismology and noise under the ocean, *Rev. Geophys.*, *36*, 105–142, doi:10.1029/97RG02287.
Weichert, D. H., and M. Henger (1976), The Canadian seismic array monitor processing system (CANSAM), *Bull. Seismol. Soc. Am.*, *66*, 1381–1403.